

## REPORT No. 464

# NEGATIVE THRUST AND TORQUE CHARACTERISTICS OF AN ADJUSTABLE-PITCH METAL PROPELLER

By EDWIN P. HARTMAN

### SUMMARY

*This paper presents the results of a series of negative thrust and torque measurements made with a 4 foot diameter model of a conventional aluminum-alloy propeller. The tests were made in the 20-foot propeller-research tunnel of the National Advisory Committee for Aeronautics.*

*The propeller was tested for thrust and torque through a blade-angle range from  $22^\circ$  to  $-23^\circ$  at 0.75 radius and a  $V/nD$  range from zero to infinity, while mounted in front of a cowled radial-engine nacelle. With this arrangement the drag of the propeller was also measured through a blade-angle range from  $0^\circ$  to  $90^\circ$  while locked in a vertical position. Additional tests were made with the propeller and nacelle located in two positions with respect to both a monoplane wing and a biplane cellule, in which smaller ranges of blade angles and values of  $V/nD$  were covered.*

*The results show that the negative thrust is considerably affected by the shape and size of the body behind the propeller, that the maximum negative thrust increases with decrease in blade-angle setting, and that the drag of a locked propeller may be greatly reduced by feathering it into the wind. Several examples of possible applications of the data are given.*

### INTRODUCTION

Wind-tunnel tests of both model and full-scale propellers through the ordinary ranges of air velocity and revolution speed have been quite extensive. Very few tests of propellers operating under conditions of negative thrust and torque have been made, however, because conditions of negative thrust and torque are encountered only in dives and fast glides and these maneuvers in nonmilitary airplanes are relatively unimportant. The recent development of the controllable-pitch propeller has broadened the field of use for negative propeller thrust and has therefore created new interest in the subject.

In 1920, as part of a rather extensive research program on wooden propellers, Durand and Lesley ob-

tained the negative-thrust characteristics of a series of 12 wooden propellers of varying pitch, blade width, and plan form. The details of these tests may be found in reference 1. More recently the British have obtained the negative thrust and torque characteristics of a 4-bladed wooden propeller (reference 2).

Both of the above studies were narrowly limited in range of blade angles and were made without a body. Their results are therefore only indirectly applicable to flight problems.

In view of the trend in recent years toward the use of metal propellers, it seemed advisable to obtain some data on the negative thrust and torque of a conventional aluminum-alloy propeller. As the propeller is usually mounted close to a fuselage and engine, it was considered necessary to include tests with bodies comparable to those found in actual practice.

This report gives the thrust and torque characteristics of a conventional adjustable-pitch metal propeller throughout the complete  $V/nD$  range from  $V=0$  to  $n=0$ , and through a range of blade-angle settings from  $22^\circ$  to  $-23^\circ$  at 0.75 radius. The drag of a locked propeller through a blade-angle range of  $0^\circ$  to  $90^\circ$  at 0.75 radius is also given.

The greater part of this research comprises a series of tests with the propeller mounted ahead of a dummy radial-engine nacelle without wings or fuselage. Other tests, not so complete, were made with the propeller and nacelle mounted in various positions with respect to a monoplane wing and also to a biplane cellule.

Although the study is confined to one propeller and relatively few body shapes, it is believed that the data given are sufficient to enable designers to make fairly accurate calculations in most cases.

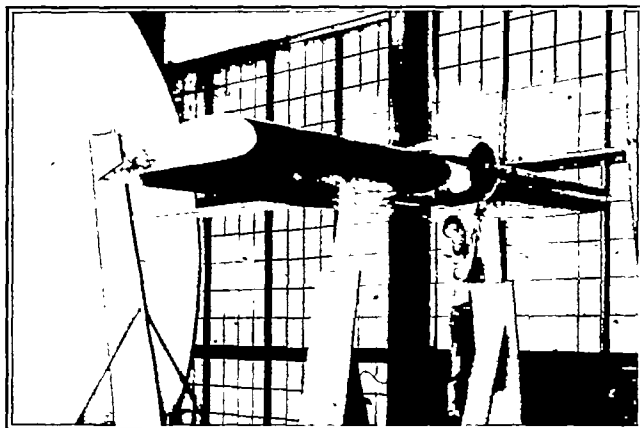
### APPARATUS AND METHODS

The tests were made in the 20-foot propeller-research tunnel of the National Advisory Committee for Aeronautics. Details of the construction and characteristics of this tunnel are given in reference 3.

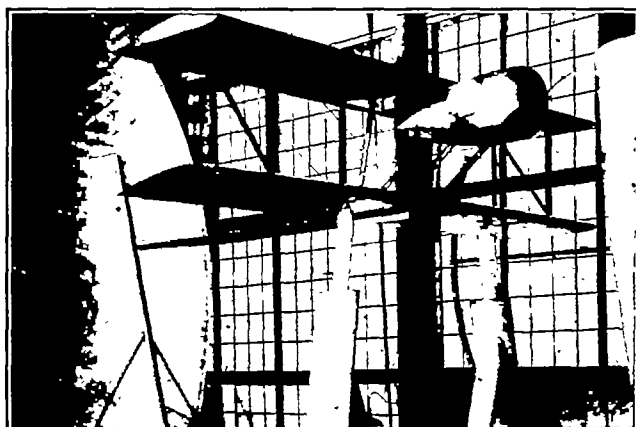
The engine-nacelle unit was composed of a 25-horsepower direct-current motor enclosed in a sheet-metal nacelle with a 4/9-scale wooden model of a Wright J-5 9-cylinder engine mounted outside at the front.



(a) Cowled engine nacelle with propeller.



(b) Nacelle mounted on monoplane wing in position A.



(c) Nacelle mounted on biplane cellule in position 9.

FIGURE 1.—Nacelle arrangements.

The motor shaft projected through the nose of the nacelle and drove a tractor propeller. In most of the tests an N.A.C.A. cowled nacelle was used. Figure 1(a) is a photograph of this nacelle mounted in testing position. Full details and dimensions may be obtained from reference 4.

The propeller-nacelle unit was tested in two positions with respect to a monoplane wing having a 15-foot span, a 5-foot chord, and a maximum thickness of 1 foot. Reference 4 gives a table of ordinates for this wing section, as well as photographs of these two monoplane-nacelle arrangements which are therein designated positions "A" and "C." The same designations will be used in this report. Figure 1(b) shows the monoplane wing with nacelle in position A.

Two biplane-nacelle arrangements, designated positions "5" and "9", were also tested. The biplane cellule had the following dimensions: Span, both wings, 15 feet 10 inches; chord, both wings, 3 feet 2 inches; gap, 3 feet; stagger, none; airfoil section, Clark Y. Figure 1(c) shows the position 9 arrangement.

The aluminum-alloy propeller used in these tests was similar to a Navy 4412 9-foot propeller, and was 4 feet in diameter, corresponding in scale to the engine and nacelle. Detailed dimensions of this propeller are given in reference 5.

The motor was made to act as an electrical brake through the negative-torque range, by means of a variable resistance in the armature circuit, the amount of resistance determining the speed of revolution. The field current was held constant at a predetermined value and the armature current measured. The motor having been previously calibrated both as a motor and as a generator, the input or output power was easily calculated.

The revolution speed of the propeller was measured by a condenser-type electrical tachometer mounted on the rear of the motor housing and connected by wires to an indicating instrument on the floor below.

For the purpose of obtaining test points throughout the full  $V/nD$  range, both the tunnel air speed and the propeller revolution speed were varied through wide ranges. The propeller speed varied from 0 to 3,500 r.p.m., and the tunnel air speed from 0 to 100 miles per hour. As previously mentioned, the more complete tests in this program were made with the cowled nacelle alone, in which propeller blade-angle ranges of  $22^\circ$  to  $-23^\circ$  with propeller free and  $0^\circ$  to  $90^\circ$  with propeller locked were covered. Tests were also made at two blade-angle settings with the hood of the N.A.C.A. cowling removed and the engine cylinders exposed. In all the tests made with the nacelle alone the thrust line was parallel to the wind direction.

The propeller was tested at four blade angles,  $22^\circ$ ,  $17^\circ$ ,  $12^\circ$ , and  $7^\circ$  at 0.75 radius, with the nacelle in position A, and at two blade angles,  $22^\circ$  and  $17^\circ$  at 0.75 radius, with the nacelle in positions C, 5, and 9. The latter three tests were made at two angles of attack,  $-5^\circ$  and  $0^\circ$ , whereas all of the other tests in this report were made at  $0^\circ$  only. The monoplane and biplane tests were limited to the negative thrust and torque range.

In each test the drag or thrust, torque, propeller revolution speed, and air speed were determined over

the desired range from readings of the balances, ammeters, and manometer.

### RESULTS

Two forms of coefficients were used in plotting these data. In the majority of the tests the coefficients  $T_c = \frac{T_c}{\rho V^2 D^3}$  and  $Q_c = \frac{Q}{\rho V^2 D^3}$  were used, since they are better adapted to plotting in the range of high  $V/nD$  values, where negative propeller thrust usually occurs. In the tests with the nacelle alone, however, where the full range of  $V/nD$  was covered, it was found necessary to use the coefficients  $C_T = \frac{T_c}{\rho n^2 D^4}$  and  $C_Q = \frac{Q}{\rho n^2 D^5}$  in the range of low  $V/nD$  values.

The significance of the units in these coefficient forms is as follows:

$T$ , thrust of propeller (tension in propeller shaft)

$\Delta D$ , change in drag of the airplane due to propeller slipstream

$T_e$ , effective thrust =  $T - \Delta D$

$Q$ , aerodynamic torque. Negative torque is defined as an air reaction upon the propeller tending to assist the rotation. Positive torque, which is the reaction occurring in normal flight, tends to resist rotation.

$D$ , propeller diameter

$n$ , revolutions per unit of time

$\rho$ , mass density of the air

all values being expressed in consistent units.

It is clear that one form of the coefficients given may be changed to the other by multiplying or dividing by  $(V/nD)^2$ .

Figures 2 and 3 represent the performance of a propeller throughout the complete  $V/nD$  range and through a large range of blade angles. The use of both forms of the coefficient keeps the charts within reasonable dimensions. A  $V/nD$  value of unity was used as the point of transition from one form of coefficient to the other because both have equal values at that point.

Figure 4 was obtained by cross-plotting some of the curves from figures 2 and 3, and replotting. It was designed primarily as a working chart and covers what might at this time be called the usable negative-thrust range of blade angles and  $V/nD$  ratios. The coefficients  $T_c$  and  $Q_c$  were used exclusively in this figure since their similarity to a drag coefficient renders them suitable for use in performance calculations.

Figures 5 and 6 present the results of the tests with the monoplane wing, and figures 7 and 8 those with the biplane cellule. Figure 9 shows the curves for the propeller mounted on the nacelle alone both with and without the engine cowling; and in figures 10 and 11 composite curves show the comparative

performances of the propeller with various wing-nacelle combinations. The drag coefficient for a locked propeller set at any blade angle between  $0^\circ$  and  $90^\circ$  is given in figure 12.

### DISCUSSION

The negative-thrust curves in this report are very similar in shape to those given in references 1 and 2. On account of the small amount of available data on negative propeller thrust, all comparisons are confined to the data given in this report.

The curves in figures 2 and 3 cover every condition that an airplane would ever encounter in flight. On the left halves of the charts in their normal positions are plotted  $C_T$  and  $C_Q$ , respectively, and on the right halves the alternative coefficients  $T_c$  and  $Q_c$ , respectively. If it be desired to extend either set of coefficients beyond the center line, it is only necessary to divide by the square of the abscissa.

The curves in figure 4 are taken from figures 2 and 3. From them it appears that in the range of blade angles covered in these tests, the maximum negative thrust coefficient increases with a decrease in blade angle. Inasmuch as the drag of an idling propeller depends upon its speed of revolution, which in turn depends upon the torque of the engine, it is essential that curves of torque coefficients should be included in any working chart. Congestion is avoided in this chart by limiting the range of blade angles and  $nD/V$  to that portion which is most likely to be of use.

The curves in figures 5 and 6, for the nacelle mounted on the monoplane wing, have the same general shape as those for the nacelle alone, but show somewhat lower values. Figure 6 indicates that small changes in angle of attack have but slight effect on the propeller drag.

The results of the tests with the biplane arrangements in figures 7 and 8 show no material differences from the other test results. The effect of removing the cowling is indicated in figure 9. The curves show that this effect is not large, and also show that a difference in negative thrust coefficients is not always accompanied by a difference in the corresponding torque coefficients.

Figures 10 and 11 present a composite of curves taken from the previous plots for the purpose of comparing the results from various wing-nacelle arrangements. These curves indicate that, in general, the larger the obstruction and the closer its position behind the propeller the less the negative thrust of the propeller. The thrust and torque curves vary in approximately the same manner. Considerable variation in the  $V/nD$  for zero thrust is noted. It is evident from these charts that body effect must be considered for accurate performance calculation.

The curve in figure 12 shows that a remarkable saving in drag may be effected by feathering the

blade of a locked propeller into the wind. The drag coefficient  $T_c$  drops from 0.0227 at  $22^\circ$  to 0.0014 at  $88^\circ$ .

**APPLICATIONS**

Only recently has any attempt been made to put negative propeller thrust to use. The development and more general use of the controllable-pitch propeller have brought about a new interest in this subject, and

tude rapidly, the dive speeds of modern airplanes have reached such high values as to make it difficult for the pilot to maintain satisfactory control of his airplane. In such cases it is desirable to provide a means by which the pilot, if he wishes, may reduce its terminal velocity.

It has been proposed that the high drag of a propeller set at low blade angles be used to reduce terminal

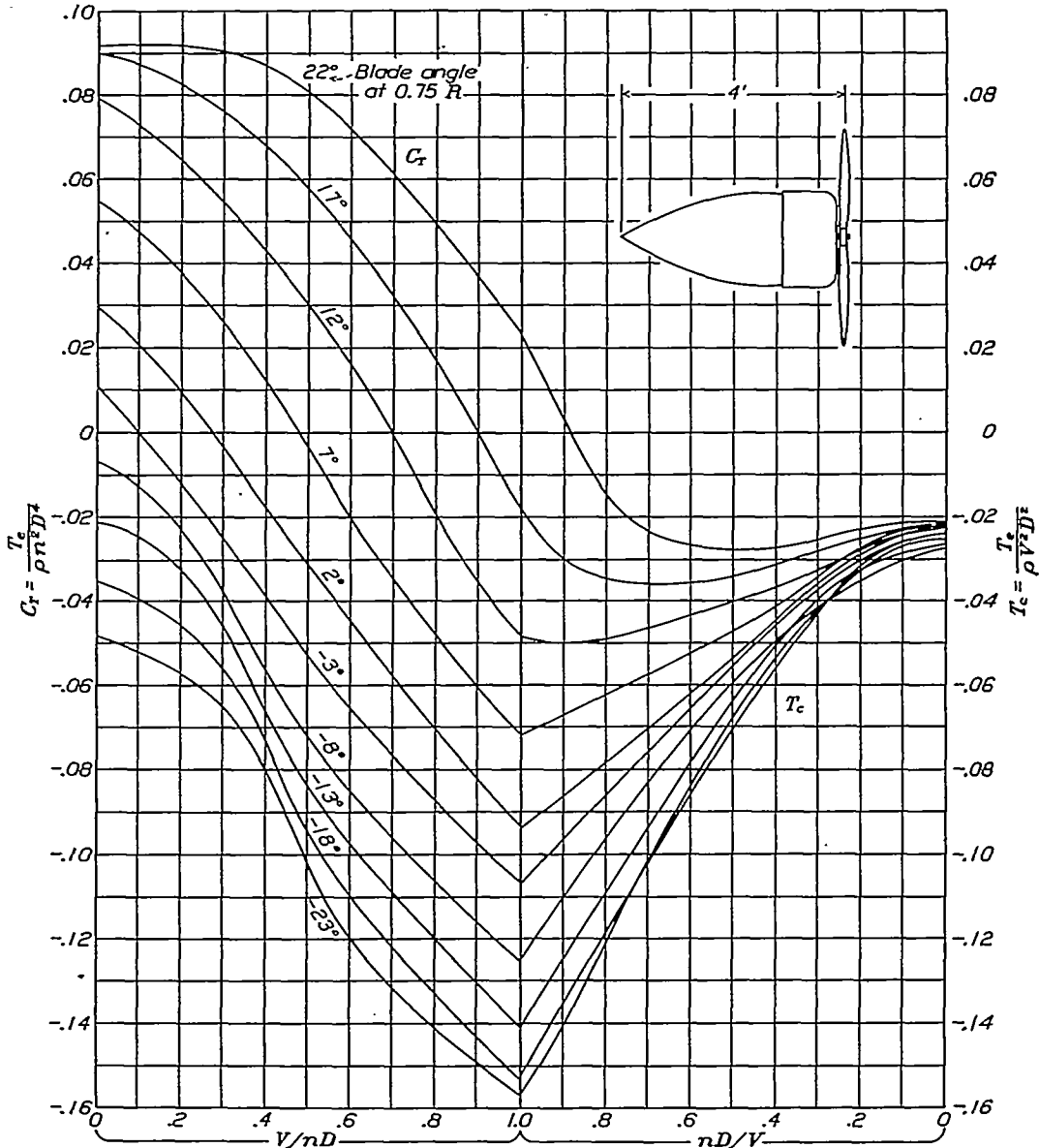


FIGURE 2.—Thrust coefficients for propeller with nacelle alone.

requests for negative-thrust data for aluminum-alloy propellers have become more frequent. Some of the applications of the data are discussed in the following paragraphs.

**REDUCTION OF TERMINAL VELOCITY**

Airplanes, particularly those used by the military services, are frequently required to dive to terminal velocity in order to carry out their specified missions. Although the purpose of this maneuver is to lose alti-

velocities, both to provide better control in the dive and to lessen the strain on both airplane and pilot in the dive and the subsequent pull-out. This procedure, of course, requires the use of a controllable-pitch propeller.

Figure 13 presents graphically the results of terminal-velocity calculations for a conventional biplane. The calculations were made using the data in figure 4; as body or high-tip-speed effects were not considered no pretension to great accuracy is made. The short

portions of the curves were calculated for the condition where engine power was used to maintain the propeller revolution speed at 2,200 r.p.m. In this way the terminal velocity is reduced much more than when the engine is fully throttled.

In making these calculations the equation used to compute the terminal velocity was

$V_T$ , terminal velocity in feet per second  
 $\rho$ , air density in slugs per cubic foot.

A curve of friction torque plotted against revolution speed of the engine is necessary for these calculations.

An approximate method of making terminal-velocity calculations is as follows:

1. Select a propeller-blade angle and diameter

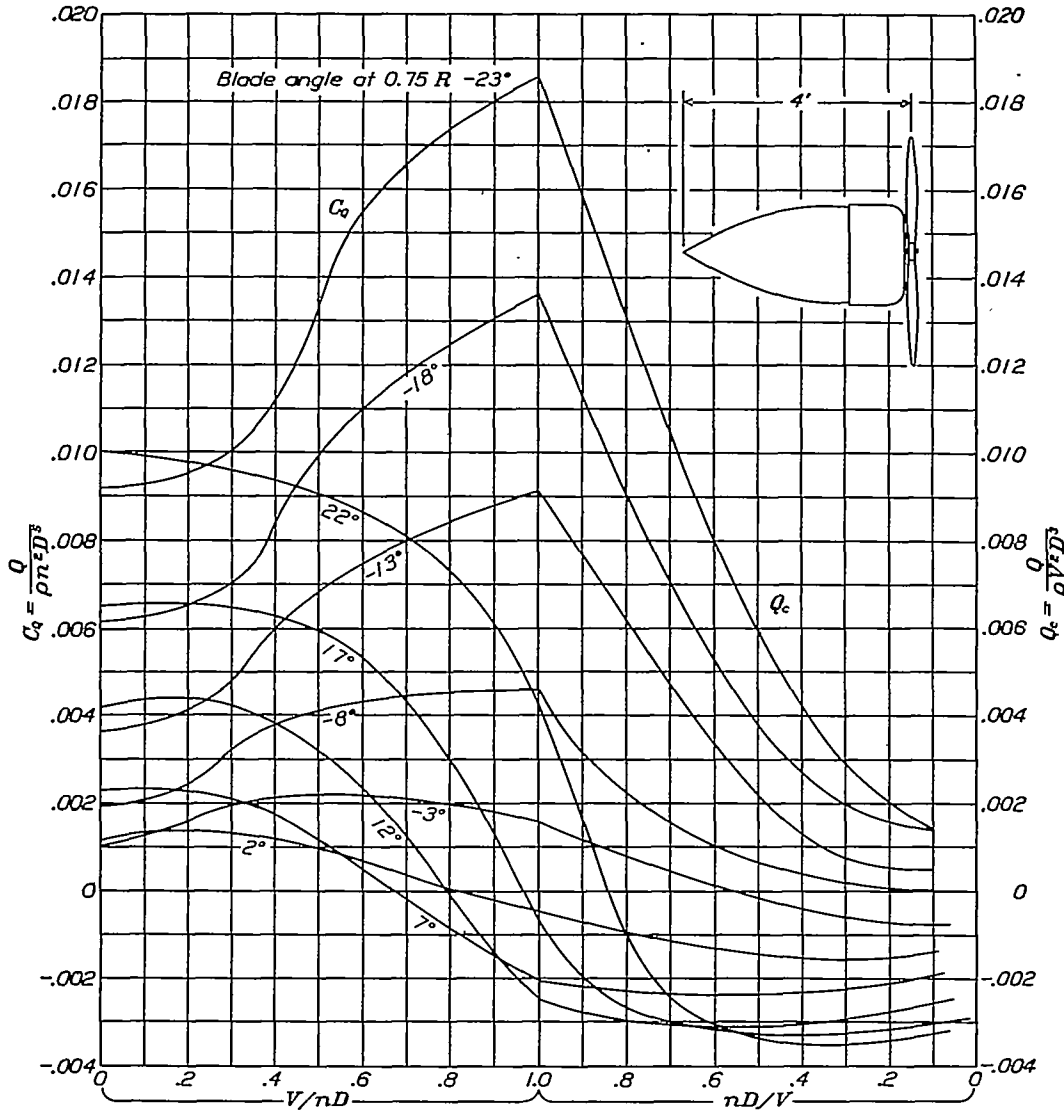


FIGURE 3.—Torque coefficients for propeller with nacelle alone.

$$V_T = \sqrt{\frac{W}{\frac{\rho}{2} A + K T_c}}$$

where

$W$ , the weight of the airplane

$A = \frac{\text{parasite drag of airplane}}{\frac{\rho}{2} V^2}$ , an equivalent parasite area

site area

$T_c$ , the propeller-thrust coefficient taken from the charts

$K = \rho D^3$

$D$ , propeller diameter in feet

2. Estimate  $V_T$  and propeller speed at  $V_T$ .

3. Using estimated propeller speed, obtain friction torque from curve of friction torque against propeller speed, which is assumed to be available.

4. Calculate  $Q_c$  from known values of friction torque and  $V_T$ .

5. Project down from value of  $Q_c$  on curves and obtain  $T_c$  and  $nD/V$ .

6. Substitute value of  $T_c$  in equation and calculate  $V_T$ .

7. Knowing  $D$  and  $nD/V$ , calculate propeller speed using calculated value of  $V_T$ .

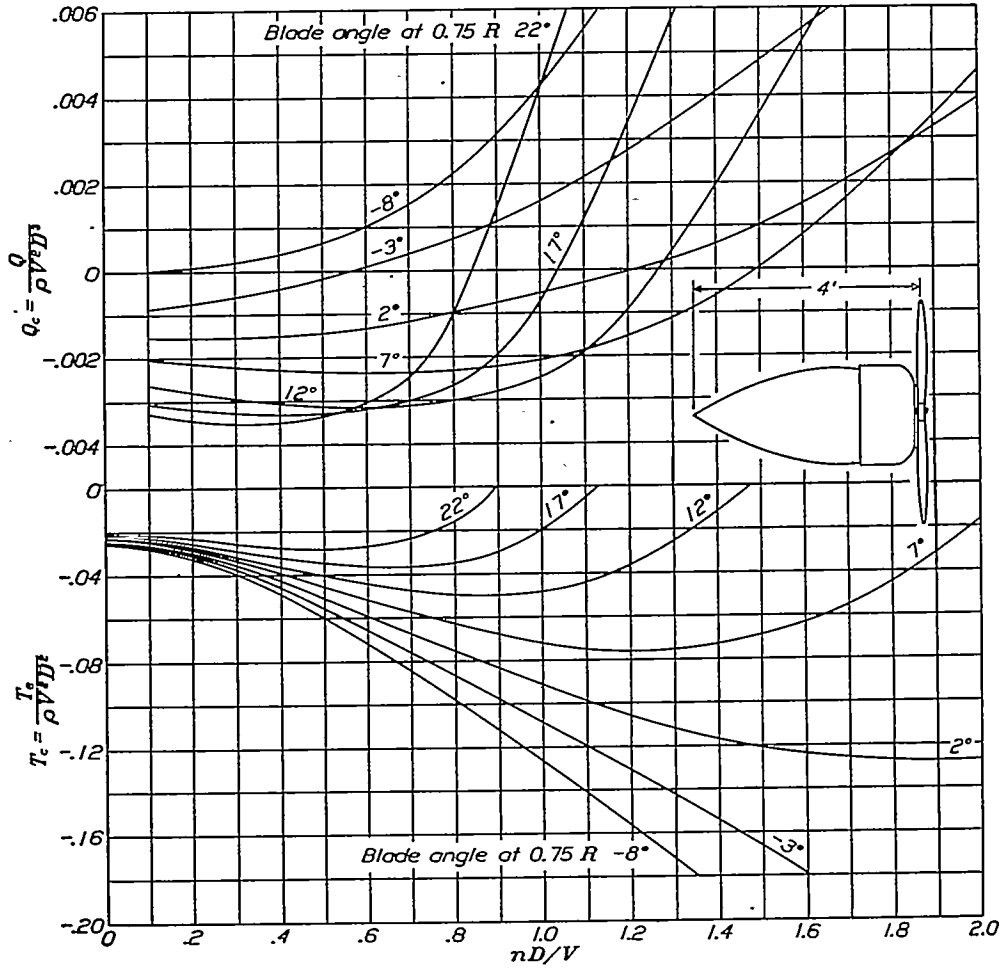


FIGURE 4.—Negative thrust and torque coefficients with nacelle alone.

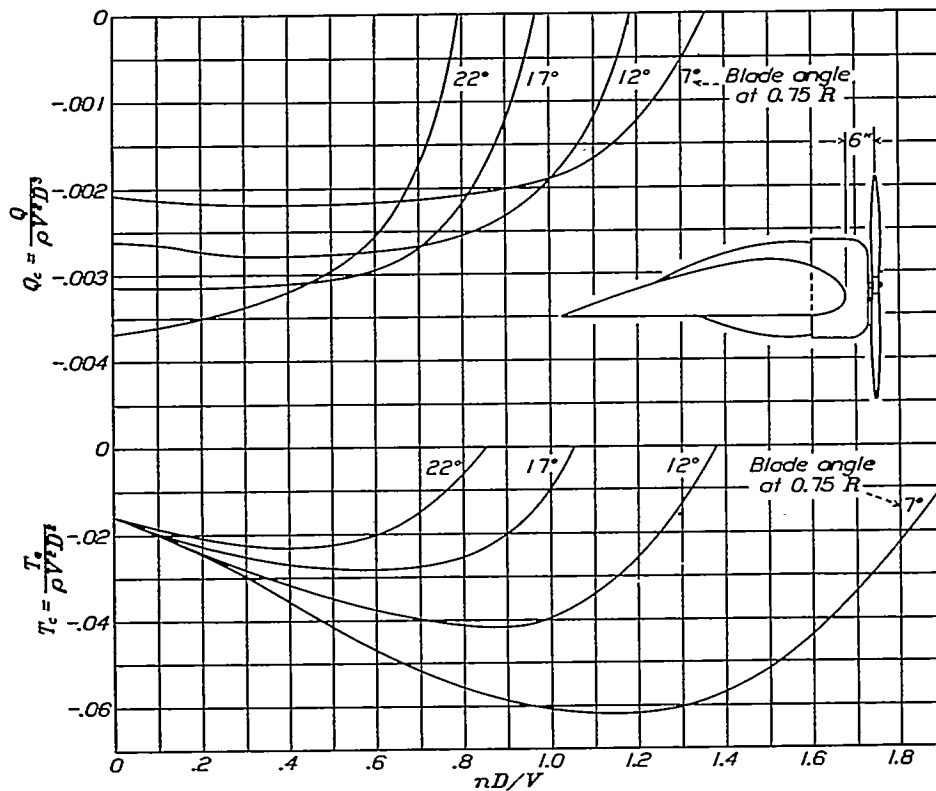


FIGURE 5.—Negative thrust and torque coefficients with monoplane wing, nacelle in position A.

8. If the calculated values of  $V_T$  and propeller speed are not the same as the estimated values, a new estimate must be made and the process repeated.

If the propeller is not of the same form as the one used in these tests, an adjustment of the data will of course be necessary. For greater accuracy high-tip-speed and body effects must also be considered. The effect of high tip speeds may be determined from data given in reference 6.

The results of the terminal-velocity calculations given in figure 13 show that as the propeller pitch is

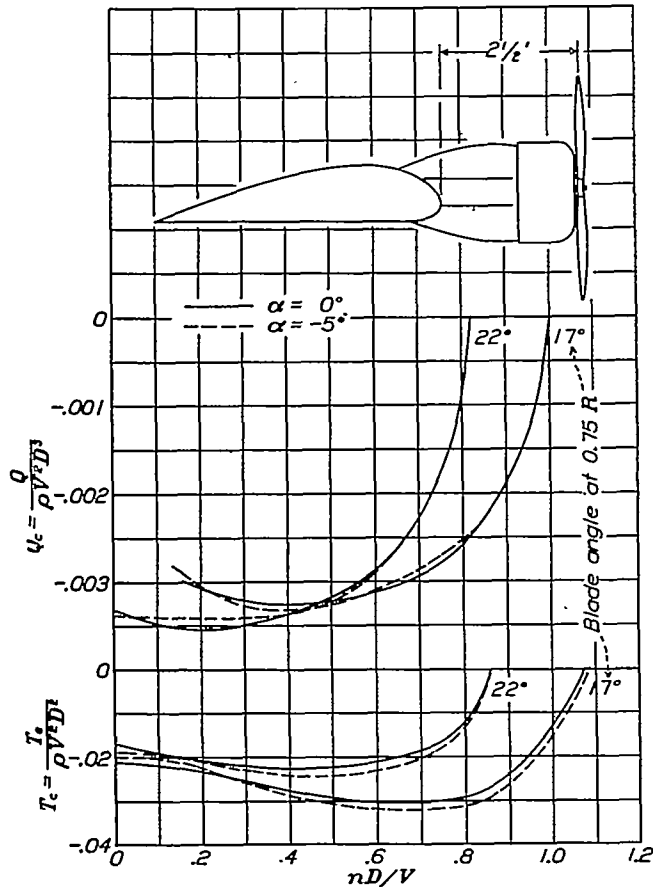


FIGURE 6.—Negative thrust and torque coefficients with monoplane wing, nacelle in position O.

reduced the terminal velocity drops rapidly to a point where the blade angle is about  $4^\circ$  at 0.75 radius, after which, with further decrease of pitch, it rises unless the revolution speed of the propeller is maintained by the use of engine power.

The flight-research section of the National Advisory Committee for Aeronautics has recently completed a series of terminal-velocity dive tests upon a military airplane equipped with a Hamilton Standard controllable-pitch propeller. The results of these tests when published will give more exact information concerning the effect of propeller-blade angle upon diving velocities.

**BRAKING EFFECT**

The braking effect of the propeller may be used to reduce the landing distance required by an airplane in the following ways:

1. To increase the angle of descent.
2. To counteract the floating tendency of clean airplanes.
3. To reduce the landing run.

In landing, a high-pitch propeller produces considerable thrust even at low engine revolution speeds. The thrust may be greatly reduced by decreasing the blade angle and the extreme braking effect may be

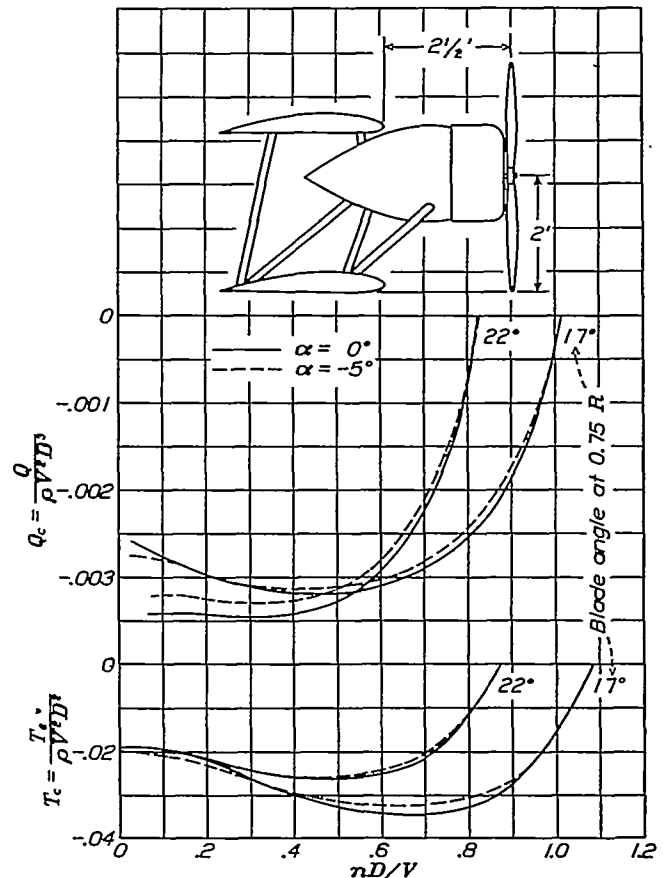


FIGURE 7.—Negative thrust and torque coefficients with biplane cellule, nacelle in position 9.

obtained by reducing the blade angle to a high negative value and applying engine power to maintain a  $V/nD$  giving the greatest negative thrust. In actual practice this might be a dangerous procedure if the airplane were not safely on the ground. In the glide before landing it would hardly be safe to reduce the blade angle below a value giving sufficient performance to enable the airplane to pull off the field again in case of an emergency.

The accurate calculation of the effect of propeller braking upon the landing run is altogether too lengthy to be of practical use; however, an estimate may be

made using the landing-run formula for still air given by Glauert (reference 7):

$$\text{Landing run in feet, } S = \frac{V_L^2}{2g \left( \frac{D}{L} - \mu \right)} \log_e \left( \frac{D}{L} \right)$$

where  $V_L$  is the landing speed in feet per second;  $\frac{D}{L} = \frac{C_D}{C_L}$  is the value of these ratios in the landing attitude; and  $\mu$  is the coefficient of friction between the landing gear and the ground.

Assuming a given reduction in blade angle, an equivalent additional  $\Delta C_D$  may be calculated using

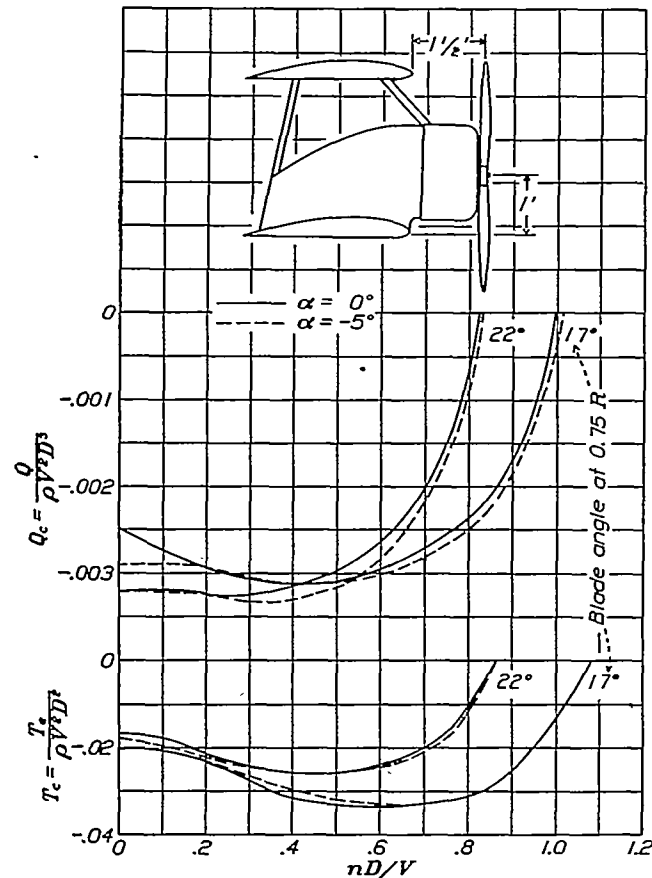


FIGURE 8.—Negative thrust and torque coefficients with biplane cellule, nacelle in position 5.

curves in figure 2 and the known characteristics of the airplane. The new value of  $D/L$  is  $\frac{C_D + \Delta C_D}{C_L}$ . It is then easy to calculate the length of landing run for each blade angle using the two values of  $D/L$ .

The additional-drag coefficient  $\Delta C_D$  varies considerably with  $V/nD$ , which makes it necessary to use an average value to avoid a lengthy integration. The use of an average coefficient may involve some error but it is believed that a close approximation to the correct results may be obtained if the  $\Delta C_D$  used is calculated for the  $V/nD$  that exists at the beginning of the landing run. The calculation of  $\Delta C_D$  is merely a transformation from  $T_c$ .

As an illustration, consider the example of an airplane with the following characteristics: Landing speed, 88 feet per second; a 9-foot diameter controllable-pitch propeller with a normal high-speed setting of  $22^\circ$ ; wing area of 250 square feet; a  $D/L$  or  $C_D/C_L$  ratio in the landing position of 0.125. For convenience a value of  $\mu$  of 0.10 will be used.

The lift coefficient  $C_L$  in the landing position will be about 1.4, so that  $C_D = 1.4 \times 0.125 = 0.175$ . If it is assumed that the blade angle for landing has been reduced to  $7^\circ$ , the average additional-drag coefficient  $\Delta T_c$  is about 0.125.

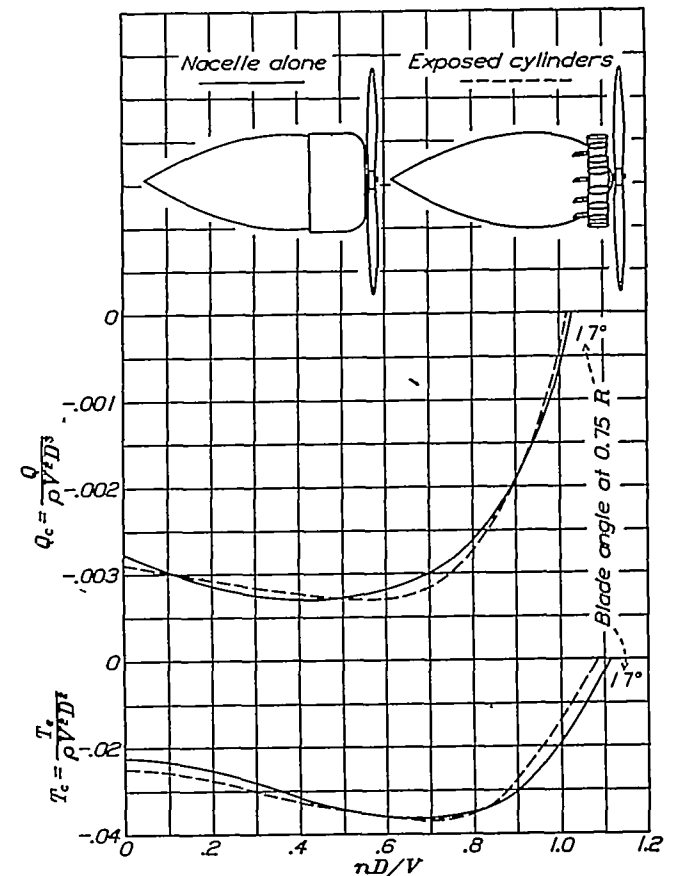


FIGURE 9.—Negative thrust and torque coefficients with nacelle alone, both with and without the engine cowling.

The relation between  $C_D$  and  $T_c$  is:

$$\frac{C_D}{T_c} = \frac{2D^2}{S_w} = \frac{2 \times 9^2}{250} = 0.648$$

The drag coefficient  $\Delta C_D$  corresponding to the additional-drag coefficient  $\Delta T_c$  is  $0.648 \times 0.125 = 0.081$ . The total drag coefficient in the  $7^\circ$  position will be  $0.175 + 0.081 = 0.256$ . The  $D/L$  ratio for the  $7^\circ$  condition will be  $\frac{0.256}{1.4} = 0.183$ .

If we consider that Glauert's formula using the original value of  $D/L$  gives the correct landing run with the blade at  $22^\circ$ , then the landing run with a  $7^\circ$  blade setting may be obtained by using the new value of  $D/L$ .

The solution for each blade angle gives 1,080 feet for the 22° setting and 880 feet for the 7° setting, the ratio of the two landing runs being 0.82. The reduction in landing run is perhaps a trifle optimistic because of the low  $D/L$  assumed for the 22° blade setting, for it is evident that the cleaner the airplane the greater will be the benefit derived from a reduction in blade angle.

The ratio of the  $L/D$  ratios in the landing position for the two blade settings is then  $\frac{0.125}{0.183} = 0.68$ . It is evident that the reduction in the  $L/D$  ratio will not only increase the glide angle but should also effectively eliminate any floating tendency. The combination of these effects should materially reduce the length of runway required. The fact that any air-

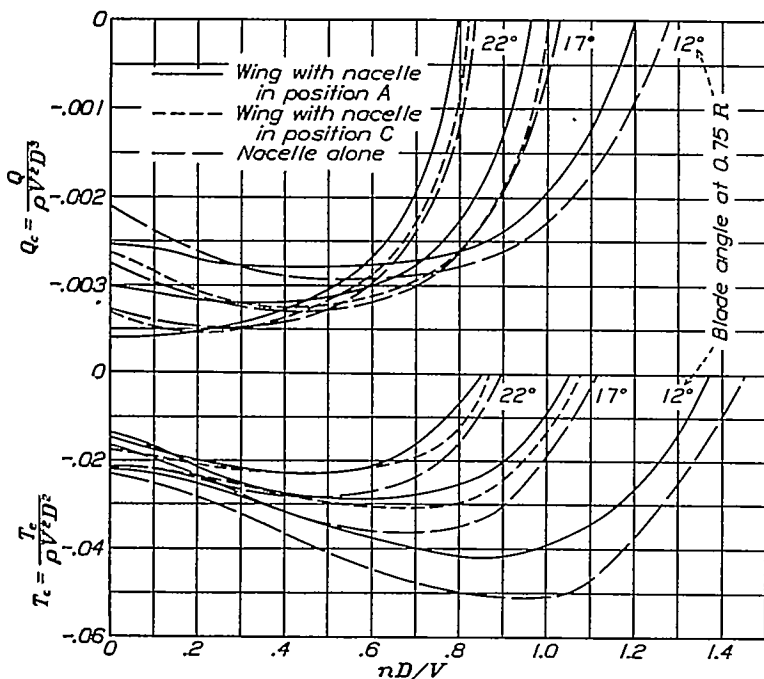


FIGURE 10.—Negative thrust and torque coefficients, nacelle mounted on monoplane wing—composite curves.

plane with a controllable-pitch propeller is very probably equipped with brakes tends to minimize the value of the propeller braking effect in shortening the landing run.

**DRAG OF LOCKED, IDLING, AND FREE-WHEELING PROPELLERS**

For the purpose of reducing the drag of an idling propeller it has often been proposed that a "free-wheeling" clutch be placed upon the propeller shaft so that the propeller might be disengaged from the engine while the engine is not in operation. Using such a device a multi-engined airplane after reaching its cruising altitude could, it has been proposed, have one or more engines stopped and could cruise more economically under reduced power. It has also been proposed that in case controllable-pitch propellers were being used the dead-engine propellers might be feathered into the wind and locked, thus effecting an

additional saving. There has been some doubt as to whether a free-wheeling propeller actually has less drag than a locked or idling propeller.

Using the data in figure 4, such problems may be solved. The drag of a locked propeller is easily found, since the drag coefficient remains constant and is equal to the thrust coefficient at  $\frac{nD}{V} = 0$ . The coefficient may be quickly found from figure 12. The drag

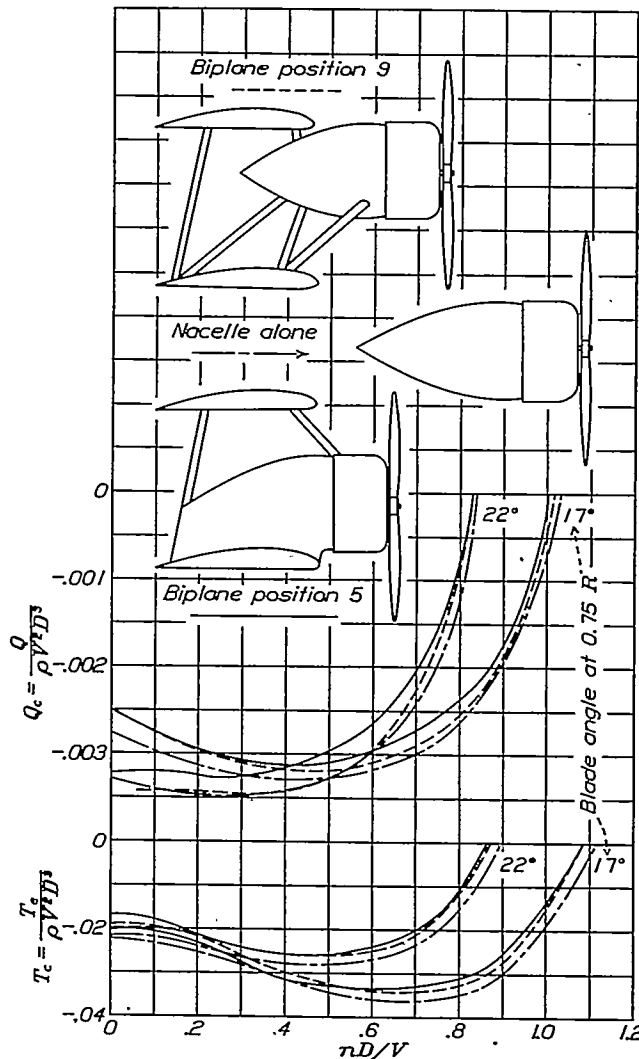


FIGURE 11.—Negative thrust and torque coefficients, nacelle mounted on biplane cellule—composite curves.

coefficient of a free-wheeling propeller also remains constant since the propeller is operating at nearly zero torque. It may be found by projecting down from the point of zero torque to the appropriate thrust curve. From an observation of the free-wheeling propeller-thrust coefficients for various blade angles in figure 4, it is noted that, for blade angles of more than 15° at 0.75 radius, the drag of a free-wheeling propeller is slightly less than the drag of a locked propeller, whereas for blade angles less than 15° the drag of a free-wheeling propeller is more than that of a locked propeller.

The drags of dead-engine idling and throttled-engine idling propellers are much more difficult to calculate

because the thrust coefficient is different for each velocity. A friction-torque curve for the engine must be at hand because the speed of rotation of the propeller, therefore the thrust coefficient, depends upon the friction in the engine. In addition to the friction-torque curve a throttled-power curve must be had for the calculation of the drag of a throttled-engine idling propeller. These data being available, the determination of propeller drag for the idling propellers resolves itself into a cut-and-try process.

The results of calculations for a typical example follow. The airplane in this example is assumed to have a 250-horsepower engine. Friction-torque and throttled-power curves for this engine were assumed but will not be shown here.

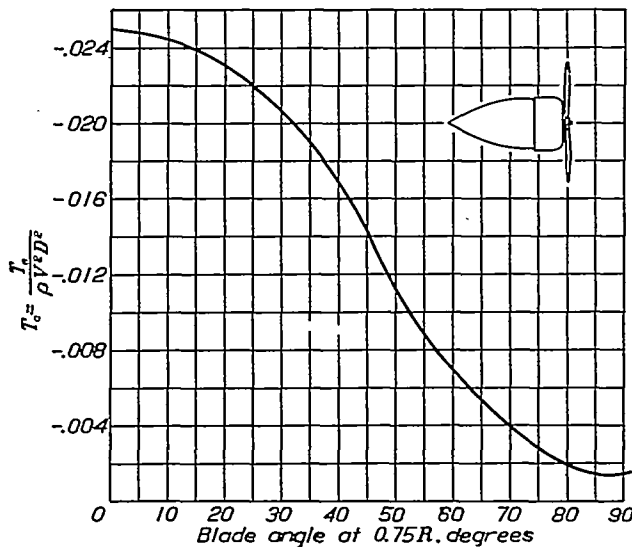


FIGURE 12.—Variation of negative-thrust coefficient with blade-angle setting for a locked propeller.

**DRAG OF LOCKED, FREE-WHEELING, AND IDLING PROPELLERS**

Propeller No. 4412—Diameter, 9 feet  
 Drag in pounds

Velocity, m.p.h.	Locked propeller set 17°	Locked propeller set 88°	Free- wheeling propeller set 17°	Dead-en- gine propeller set 17°	Throttled- engine propeller set 17°
25	5.9	0.36	3.7	5.9	-22
50	23.6	1.5	15.0	37.2	22
75	53.0	3.3	33.7	68.6	60
100	94.4	5.8	60.1	101.0	100

The throttled engine was assumed to be throttled to a point giving 350 r.p.m. at zero velocity. From this table it appears that in most cases a free-wheeling propeller would have some advantage over a locked or an idling propeller, except where the blade of the locked propeller has been feathered into the wind.

In this example the dead-engine idling propeller absorbs 27 horsepower at 100 miles per hour; the free-wheeling propeller, 16 horsepower; and the locked propeller set 88°, only 1½ horsepower.

At some speed between 25 and 50 miles per hour the aerodynamic torque of the dead-engine propeller becomes insufficient to overcome the friction torque of the engine, and the propeller stops. Below this speed the drag is the same as that for a locked propeller.

Although the number of uses for negative propeller thrust has been greatly increased by the development of the controllable-pitch propeller, the uses are still relatively few. An attempt has been made in the preceding paragraphs to indicate some of the problems in this field and to show how the data in this report may be used in their solution.

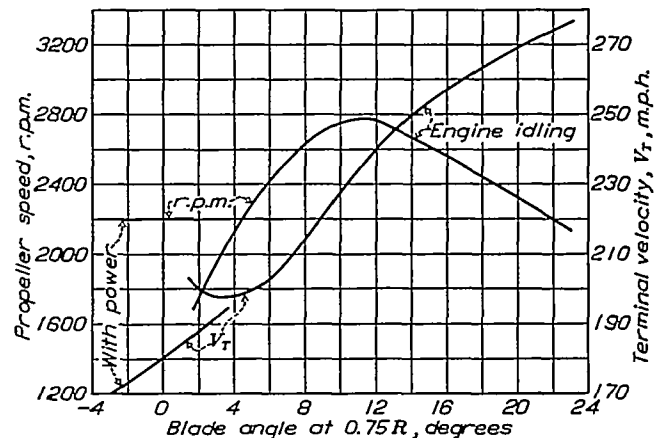


FIGURE 13.—The performance in a terminal-velocity dive of an airplane having the following characteristics: Gross weight, 2,630 pounds; engine, 420 horsepower at 2,200 r.p.m.; propeller, 4412, diameter 9 feet. Equivalent parasite area ( $D_p/q$ ) 11.4 square feet.

**CONCLUSIONS**

1. The negative thrust of a propeller is considerably affected by the shape and size of the body behind it.
2. Through the range of blade angles covered in these tests, the maximum negative-thrust coefficient increases with decrease in blade angle.
3. For blade angles below 7° it is necessary to use engine power to obtain the greatest negative thrust.
4. The drag of a free-wheeling propeller is slightly less than that of a locked propeller in the normal range of blade-angle settings.
5. The drag of a locked propeller may be greatly reduced by feathering it into the wind.

LANGLEY MEMORIAL AERONAUTICAL LABORATORY,  
 NATIONAL ADVISORY COMMITTEE FOR AERONAUTICS,  
 LANGLEY FIELD, VA., May 23, 1933.

**REFERENCES**

1. Durand, William F., and Lesley, E. P.: Experimental Research on Air Propellers, II. T.R. No. 30, N.A.C.A., 1920.
2. Lock, C. N. H., and Bateman, H.: Airscrews at Negative Torque. R. & M. No. 1397, British A.R.C., 1931.

3. Weick, Fred E., and Wood, Donald H.: The Twenty-Foot Propeller Research Tunnel of the National Advisory Committee for Aeronautics. T.R. No. 300, N.A.C.A., 1928.
4. Wood, Donald H.: Tests of Nacelle-Propeller Combinations in Various Positions with Reference to Wings. Part I. Thick Wing—N.A.C.A. Cowled Nacelle—Tractor Propeller. T.R. No. 415, N.A.C.A., 1932.
5. Weick, Fred E.: Working Charts for the Selection of Aluminum Alloy Propellers of a Standard Form to Operate with Various Aircraft Engines and Bodies. T.R. No. 350, N.A.C.A., 1930.
6. Wood, Donald H.: Full-Scale Tests of Metal Propellers at High Tip Speeds. T.R. No. 375, N.A.C.A., 1931.
7. Glauert, H.: The Landing of Aeroplanes (Part I). R. and M. No. 666 British A.C.A., 1920.